labeled complex exist. As was the case for ci-trans isomerization via h_1^{WV}, the identities of the a-a and e-e isomers merge while that of the a-e isomer remains distinct. The final conclusion, therefore, is that no single cis-trans isomerization mechanism can lead to interconversion of all three permutational isomers of a rigid *cis*-$M(A\text{-}A')_2B_2$ complex, assuming of course that cis-trans isomerization does not involve any further symmetric intermediate configurations having connectivities greater than two.

For the general case of generating a complete set of permutational isomers of a partially labeled compound having geometry *V*, one must proceed in the following manner:

1. Label the nuclear sites in all relevant configurations.
2. Label the nuclei which may occupy them.
3. Define and read into the computer the permutations in the proper configurational symmetry group V^{VV}, an improper configurational symmetry operation v'^{VV} (if the molecule has an achiral skeleton), the nuclear symmetry group *L*, and the group of allowed permutations H^{VV}.
4. Read in the statement "ISOCNT *V, H, L, V*PRIME". If the molecule has a chiral skeleton and v'^{VV} is undefined, the permutation v'^{VV} is omitted from the input.

Supplementary Material Available: Complete description of the dynamic stereochemistry program and instructions for its use (23 pages). Ordering information is given on any current masthead page.

References and Notes

(1) Parts 1 and 2 of this series: W. G. Klemperer, *J. Am. Chem. Soc.*, **95**, 380–396, 2105–2120 (1973).
(2) (a) University College London; (b) Columbia University; (c) Princeton University Computing Center.
(3) (a) W. G. Klemperer, *J. Chem. Phys.*, **56**, 5478–5489 (1972); (b) *Inorg. Chem.*, **11**, 2668–2678 (1972); (c) *J. Am. Chem. Soc.*, **94**, 6940–6944 (1972); (d) *ibid.*, **94**, 8360–8371; (e) W. G. Klemperer in "Dynamic Nuclear Magnetic Resonance Spectroscopy", L. M. Jackman and F. A. Cotton, Ed., Academic Press, New York, N.Y., 1975, pp 23–44.
(4) (a) E. L. Muetterties, *J. Am. Chem. Soc.*, **91**, 1636–1643 (1969); (b) P. Meakin, E. L. Muetterties, F. N. Tebbe, and J. P. Jesson, *ibid.*, **93**, 4701–4709 (1971).
(5) (a) E. Ruch, W. Hasselbarth, and B. Richter, *Theor. Chim. Acta*, **19**, 288–300 (1970); (b) W. Hasselbarth and E. Ruch, *ibid.*, **29**, 259–267 (1973).
(6) C. K. Johnson and C. J. Collins, *J. Am. Chem. Soc.*, **96**, 2514–2523 (1974).
(7) (a) J. G. Nourse and K. Mislow, *J. Am. Chem. Soc.*, **97**, 4571–4578 (1975); (b) J. G. Nourse, *Proc. Natl. Acad. Sci. U.S.A.*, **72**, 2385–2388 (1975).
(8) J. Brocas, *Top. Curr. Chem.*, **32**, 44–61 (1972).
(9) A complete description of the dynamic stereochemistry program DYNAMSTER employed below is given in the Appendix together with instructions for its use. See paragraph at end of paper regarding supplementary material.
(10) T. J. Katz and C. R. Renner, unpublished results.
(11) I. Ugi, D. Marquarding, H. Klusacek, G. Gokel, and P. Gillespie, *Angew. Chem., Int. Ed. Engl.*, **9**, 703–730 (1970).
(12) A convenient verballzation of an operation such as $(143)(2)^{BA}$ is "the nucleus in site 1A is moved to site 4B, the nucleus in site 4A is moved to site 3B, the nucleus in site 3A is moved to site 1B, and the nucleus in site 2A is moved to site 2B".
(13) We shall refer to reactions representing different steric courses as differentiable reactions[1] (or reactions differentiable in a chiral environment) and reactions representing the same steric course as nondifferentiable reactions[1] (or reactions nondifferentiable in a chiral environment). When treating permutational isomerization reactions, other authors have referred to a set of nondifferentiable reactions as a mode[14] or ring permutation.[15] Within their limited range of application, these terms differ in no way from the more general and precise terminology employed here.
(14) J. I. Musher, *J. Am. Chem. Soc.*, **94**, 5662–5665 (1972).
(15) J. A. Barltrop, A. C. Day, P. D. Moxon, and R. R. Ward, *J. Chem. Soc., Chem. Commun.*, 786–787 (1975), and references cited therein.
(16) W. G. Klemperer, J. K. Krieger, M. D. McCreary, E. L. Muetterties, D. D. Traficante, and G. M. Whitesides, *J. Am. Chem. Soc.*, **97**, 7023–7030 (1975).
(17) R. H. Holm, "Dynamic Nuclear Magnetic Resonance Spectroscopy", L. M. Jackman and F. A. Cotton, Ed., Academic Press, New York, N.Y., 1975, pp 333–338.

A Molecular Orbital Analysis of Electronic Structure and Bonding in Chromium Hexacarbonyl

Jeffrey B. Johnson and W. G. Klemperer*

Contribution from the Department of Chemistry, Columbia University, New York, New York 10027.

Received February 14, 1977

Abstract: The SCF-Xα-MSW method is used to calculate molecular orbitals in $Cr(CO)_6$, the ligand array $(CO)_6$, and free CO. Calculated ionization energies for $Cr(CO)_6$ and CO are compared with experiment, as are calculated electronic transition energies for $Cr(CO)_6$. Correlation of orbital energies, charge distributions, and wave function contours in these three systems leads to the conclusions that (1) metal-carbon bonding in $Cr(CO)_6$ is due primarily to Cr3d-CO5σ interactions, with only a minor contribution from Cr3d-CO2π interactions, (2) Cr4s and 4p orbitals have negligible bonding interactions with ligand orbitals, and (3) Cr3d-CO2π interactions, although weak relative to Cr3d-CO5σ interactions, play a dominant role in determining the C–O bond order in $Cr(CO)_6$ relative to free CO. Vibrational data, in particular interaction displacement coordinates, provide strong support for these conclusions.

An understanding of the interactions between carbon monoxide and transition metal atoms is essential to the understanding of structure and bonding in discrete organometallic carbonyl complexes and carbon monoxide adsorbed on metal surfaces. Chromium hexacarbonyl provides an ideal prototype system for the study of these interactions for several reasons: (1) Its octahedral symmetry implies equivalent orbital interactions at each ligand site. (2) Its symmetry also allows complete separation of metal-ligand d-σ and d-π interactions. (3) The relative simplicity of $Cr(CO)_6$ leads to photoelectron and ultraviolet spectra which are more readily interpreted than those of more complex systems. (4) A complete vibrational analysis of $Cr(CO)_6$ has been carried out which provides detailed information regarding bonding relationships in the molecule.

Molecular orbital analyses of transition metal carbonyls have traditionally followed two general approaches. Following the first approach, molecular orbitals are generated using symmetry arguments and qualitative perturbation molecular orbital theory.[1] This approach has gained wide acceptance owing to its simplicity and transferability. The principles involved are of sufficient simplicity and generality to be readily transferred from system to system. The major drawback of this approach, however, is its dependence on preconceived notions

Table I. Calculated Eigenvalues, Charge Distributions, and Ionization Energies for Carbon Monoxide Molecular Orbitals

Orbital	$-\epsilon$, eV	Charge distribution[a]				Ionization energy, eV	
		C	O	OUTS	INT	Calcd	Obsd[b]
2π	1.2	30	19	33	18		
5σ	8.5	50	8	31	12	13.5	14.0
1π	10.8	16	53	11	21	16.2	16.9
4σ	14.7	18	68	13	1	20.6	19.7

[a] Below C and O are the percentages of charge in 0.788 and 0.768 Å radii spheres about the C and O atoms, respectively; below OUTS is the percentage charge outside of a 1.342 Å radius sphere surrounding the molecule; and below INT is the percent charge in the intersphere region, defined to be the charge not accounted for in the previous columns. [b] Vertical ionization energy from ref 10.

Table II. Calculated Eigenvalues, Charge Distributions, and Ionization Energies for $(CO)_6$ and $Cr(CO)_6$ Molecular Orbitals

$(CO)_6$							$Cr(CO)_6$									
	$-\epsilon$,		Charge distribution[b]					$-\epsilon$,		Charge distribution[c]					IE, ev	
Orbital	eV	Type[a]	C	O	OUTS	INT	Orbital	eV	Type[a]	Cr	C	O	OUTS	INT	Calcd	Exptl[d]
							$2t_{1g}$	0.5	2π	0	52	20	2	26		
$8t_{1u}$	0.7		32	9	28	32	$10t_{1u}$	1.3	p	1	24	5	30	40		
							$6e_g$	1.6	d	54	16	4	5	22		
$2t_{2u}$	0.8	2π	39	21	0	39	$2t_{2u}$	1.7	2π	0	40	23	0	37		
							$3t_{2g}$	2.0	2π	23	9	16	7	46		
$7t_{1u}$	1.9	2π	14	11	19	56	$9t_{1u}$	2.6	2π	0	21	17	8	53		
$6a_{1g}$	2.3		2	1	32	64	$9a_{1g}$	2.7	s	1	3	1	28	66		
$2t_{2g}$	2.7	2π	21	24	2	53										
							$2t_{2g}$[e]	6.2	d	59	6	13	0	22	8.6	8.4
$5e_g$[e]	7.3	5σ	64	6	0	29										
$6t_{1u}$	8.8	5σ	48	18	0	34	$8t_{1u}$	9.8	5σ	5	46	23	0	26	12.1	13.4
$1t_{1g}$	10.1	1π	17	59	1	23	$1t_{1g}$	10.7	1π	0	18	58	1	23	12.9	14-16
$1t_{2u}$	10.3	1π	17	57	1	25	$1t_{2u}$	10.8	1π	0	19	55	1	25	13.1	14-16
$5t_{1u}$	10.6	1π	23	45	1	31	$7t_{1u}$	11.3	1π	2	27	39	1	32	13.5	14-16
$1t_{2g}$	10.6	1π	19	52	1	29	$1t_{2g}$	11.3	1π	2	21	47	1	30	13.4	14-16
							$5e_g$	11.3	5σ	29	45	6	0	19	13.6	14-16
$5a_{1g}$	11.5	5σ	44	10	1	46	$8a_{1g}$	12.8	5σ	10	43	13	1	33	15.0	14-16
$4e_g$	15.0	4σ	17	75	4	4	$4e_g$	15.5	4σ	0	17	74	4	5	17.8	17.8
$4t_{1u}$	15.1	4σ	17	74	3	6	$6t_{1u}$	15.6	4σ	0	16	74	3	6	17.9	17.8
$4a_{1g}$	15.1	4σ	18	71	4	7	$7a_{1g}$	15.6	4σ	1	18	68	4	9	17.9	17.8

[a] Principal metal or ligand orbital contribution. [b] Below C and O are the percentages of charge in 0.820 and 0.814 Å radii spheres about the carbon and oxygen atoms, respectively; below OUTS is the percentage charge outside of a 3.894 Å radius sphere surrounding the cluster; and below INT is the percent charge in the intersphere region, defined to be the percentage charge not accounted for in the previous columns. [c] Computed as in note *b*, where the chromium, carbon, oxygen, and outer sphere radii are 1.107, 0.814, 0.821, and 3.901 Å, respectively. [d] From ref 11c. [e] Highest occupied orbital.

regarding the relative strengths of various orbital interactions. A unique set of molecular orbitals can only be generated once the relative contributions of σ vs. π bonding, metal s, p, and d orbital participation, and metal-ligand vs. ligand-ligand interactions have been evaluated. Such a quantitative evaluation is beyond the scope of qualitative molecular orbital theory which therefore cannot uniquely generate molecular orbitals, but only present plausible bonding schemes based on various assumptions regarding the relative importance of different orbital interactions.

A second approach to molecular orbital analysis in carbonyls is based on the quantitative generation of molecular orbitals using nonempirical quantum mechanical calculations.[2] In contrast with the qualitative approach, the accuracy and hence uniqueness of these results can be assessed through a comparison of calculated electronic properties with spectroscopic data, and errors in the calculations can often be detected and corrected. Here, however, a sacrifice has been made regarding transferability. In order to transfer the insight gained into one particular molecule to a different system, one must first understand the component orbital interactions responsible for the energy and charge distribution of each molecular orbital. This has proved to be a formidable and largely unsuccessful task owing to the difficulty of isolating the large number of fundamental interactions possible in transition metal carbonyls.

In this paper we combine the above-mentioned approaches, utilizing quantitative SCF-Xα-MSW calculations not only to generate molecular orbitals, but also to isolate and assess the magnitudes of individual orbital interactions responsible for the overall molecular orbital structure. As a result, uniqueness can be assessed without sacrificing transferability. We are concerned here solely with the molecular orbitals in chromium hexacarbonyl, and will extend the results to related systems in future publications. Calculated results for CO, $(CO)_6$, and $Cr(CO)_6$ are presented, analyzed, and compared with appropriate experimental photoelectron and UV spectroscopic data. Discussion follows in three parts. First, the bonding scheme implied by the calculated results is compared with experimental data obtained from vibrational spectra. Next, the present results are compared with the results of previous theoretical studies of $Cr(CO)_6$. A brief discussion relating the present results to studies of carbon monoxide absorbed on metal surfaces follows.

Computational Procedures. All computations utilized Johnson and Slater's SCF-Xα-MSW method[3] with overlapping spheres.[4] Experimental bond distances were used for CO (d_{CO} = 1.13 Å)[5] and $Cr(CO)_6$ (d_{Cr-C} = 1.92 Å, d_{CO} = 1.17 Å)[6] calculations. The $(CO)_6$ calculation utilized the carbon and oxygen coordinates found in $Cr(CO)_6$. Atomic sphere radii (see Tables I and II) were obtained by optimizing atomic number spheres[4b] with respect to the virial ratio, obtaining $-2T/V$ = 1.0002, 1.0015, and 1.0010 for CO, $(CO)_6$, and $Cr(CO)_6$, respectively. In each case, the outer sphere was chosen to be tangent with the outermost atomic spheres. Schwartz's α_{HF} exchange parameters[7] were used in atomic

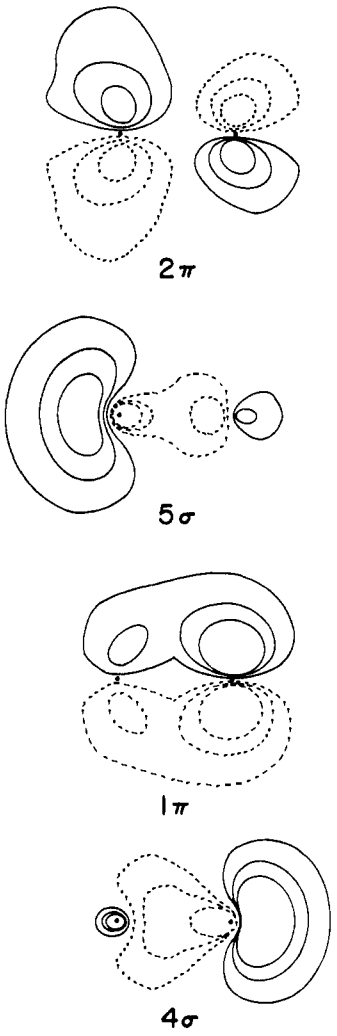

Figure 1. Wave function contours for selected carbon monoxide molecular orbitals. Solid and broken lines indicate contours of opposite sign having absolute values of 0.3, 0.2, and 0.1. The molecule is oriented with carbon on the left and oxygen on the right.

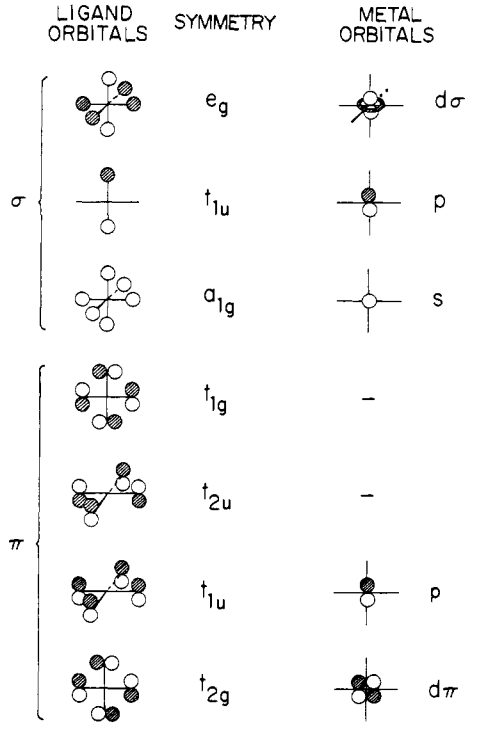

Figure 2. Octahedral symmetry adapted combinations of ligand orbitals are shown on the left, and the metal atom orbitals they may interact with are shown on the right. Only one orbital or orbital combination is shown from each degenerate set.

sphere regions and the average of the atomic values weighted according to total number of valence electrons for each type of atom was used in the outer sphere and intersphere regions. In all calculations, spherical harmonies through $l = 2$ were used in carbon and oxygen sphere regions, and functions through $l = 4$ were used in chromium and outer sphere regions. All SCF calculations were converged to better than 0.02 eV for each level with all cores relaxed. Calculated energy values have been converted from Rydberg units to electron volts (1 Rydberg = 13.6058 eV).[8]

Results

In order to separate ligand-ligand interactions from ligand-metal interactions, molecular orbitals were calculated first for an isolated CO molecule, then for the $(CO)_6$ ligand array found in $Cr(CO)_6$, and finally for the complete $Cr(CO)_6$ molecule. Calculations for a free Cr atom are not reported because chromium in $Cr(CO)_6$ has a $3d^6$ configuration whereas the free Cr atom has a $3d^54s^1$ configuration, making comparison of atomic spectroscopic data with atomic "valence state" properties meaningless. Furthermore, the large number of electronic states resulting from a $3d^6$ configuration cannot be adequately represented using one-electron molecular orbital theory as employed here.

The calculated eigenvalues and charge distributions for CO molecular orbitals (MO's) in the −0.5 to −16 eV range are tabulated in Table I and wave function contours are shown in Figure 1. When the octahedral $(CO)_6$ array is formed, CO σ and π orbitals combine to form the sets of symmetry adapted orbitals shown in the left column of Figure 2, where each set is ordered according to the number of new nodal surfaces generated. Calculated eigenvalues and charge distributions for $(CO)_6$MO's in the −0.5 to −16 eV range are tabulated in Table II, and $(CO)_6$MO's are correlated with CO MO's in Figure 3, the splittings occurring in each case according to the number of new nodal surfaces generated. Note that the CO 5σ and 2π orbitals interact strongly upon formation of $(CO)_6$, whereas the CO 4σ and 1π orbitals interact only slightly. This difference in behavior follows directly from the localization of the 5σ and 2π orbitals near carbon and the localization of the 4σ and 1π orbitals near oxygen in CO (see Table I and Figure 1). In $(CO)_6$, the carbon-carbon distances are shorter than the oxygen-oxygen distances, leading to greater interactions between orbitals localized near carbon. Of interest is the fact that the t_{1u} combination of CO 5σ orbitals may mix with t_{1u} combinations of CO 1π and CO 2π orbitals, a point which we shall return to below. Note also that the unoccupied $(CO)_6$ $6a_{1g}$ and $8t_{1u}$ orbitals, having much electron density in the outer sphere region (see Table II), arise from interactions of high-lying CO orbitals.

The symmetry allowed orbital interactions between $(CO)_6$ and Cr in $Cr(CO)_6$ are shown in Figure 2. Calculated eigenvalues and charge distributions for $Cr(CO)_6$ MO's in the −0.5 to −16 eV region are tabulated in Table II, and these orbitals are correlated with the $(CO)_6$ orbitals in Figure 3. The $2t_{2g}$, $9a_{1g}$, $6e_g$, and $10t_{1u}$ levels correlate with the chromium $3d\pi$, 4s, $3d\sigma$, and 4p orbitals, respectively. The small systematic lowering of eigenvalues in $Cr(CO)_6$ relative to $(CO)_6$ evident in Figure 3 is most probably a computational artifact resulting from the difference between sphere sizes employed in the two calculations.[9] Selected wave function contours are shown in Figure 4.

By viewing Figures 3 and 4 and consulting charge distributions tabulated in Table II, the relative magnitudes of the

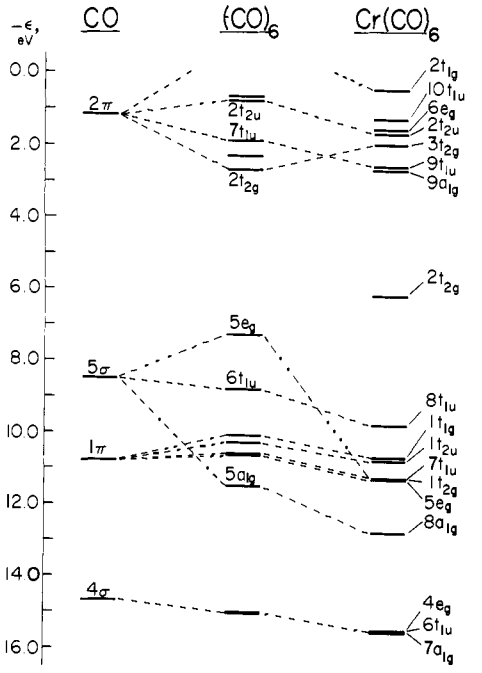

Figure 3. Molecular orbital correlation diagram indicating the parentage of $Cr(CO)_6$ orbitals from $(CO)_6$ and CO in the −0.5 to −16.0 eV orbital eigenvalue range. All orbitals with $\epsilon > -5$ eV are unoccupied.

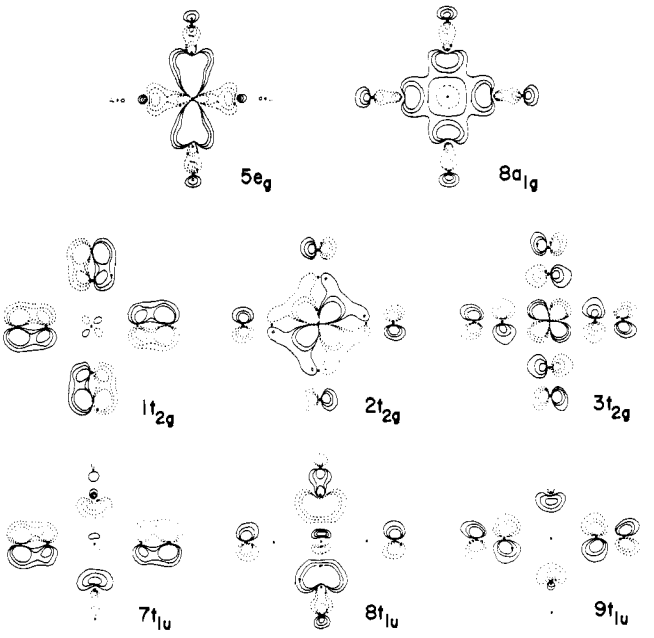

Figure 4. Wave function contours for selected $Cr(CO)_6$ molecular orbitals. Solid and broken lines indicate contours of opposite sign having absolute values of 0.100, 0.075, and 0.050. The innermost contours around Cr in the $8a_{1g}$ and $8t_{1u}$ orbitals have been omitted.

various metal-ligand interactions may be assessed. Strong σ interaction between the Cr dσ orbitals and the CO 5σ based $(CO)_6$ $5e_g$ orbitals leads to the strongly bonding $5e_g$ and strongly antibonding $6e_g$ orbitals in $Cr(CO)_6$. The strength of this interaction results in an approximately 4 eV lowering of the $Cr(CO)_6$ $5e_g$ level relative to the $(CO)_6$ $5e_g$ level. The π interaction between Crdπ orbitals and the CO2π derived $(CO)_6$ $2t_{2g}$ orbitals is apparent from the energy of the unoccupied $Cr(CO)_6$ $3t_{2g}$ metal-ligand antibonding orbitals relative to the unperturbed $(CO)_6$ $2t_{2g}$ level. The shapes of the $Cr(CO)_6$ t_{2g} orbitals shown in Figure 4 reflect the character of the various metal-ligand π interactions. As implied by simple first order perturbation theory, the $Cr(CO)_6$ $1t_{2g}$ orbital is primarily CO 1π in character, with some bonding contribution from the Crdπ orbital; the $2t_{2g}$ orbital is primarily a Crdπ orbital perturbed by bonding interaction with CO2π orbitals and antibonding interaction with CO1π orbitals; and the $3t_{2g}$ orbital is primarily CO2π in character, with antibonding contribution from a Crdπ orbital. Comparison of the $Cr(CO)_6$ $5e_g$ and $2t_{2g}$ wave function contours emphasizes the greater magnitude of Cr–C σ bonding relative to π bonding: there is far greater charge density in the Cr–C bonding region in the $5e_g$ orbital. The essentially negligible σ interaction between Cr4s and Cr4p orbitals with CO5σ derived $(CO)_6$ $5a_{1g}$ and $6t_{1u}$ orbitals is reflected in the energetic proximity of the $Cr(CO)_6$ $8a_{1g}$ and $8t_{1u}$ levels with their $(CO)_6$ counterparts. Wave function contours for the $Cr(CO)_6$ $8a_{1g}$ orbitals outline what is essentially a nodeless combination of CO5σ orbitals, only slightly perturbed by bonding interaction with the Cr4s orbital. Wave function contours for the $Cr(CO)_6$ t_{1u} levels are more complex than those of the remaining levels owing to the σ–π mixing which is allowed by symmetry: the $7t_{1u}$ level is primarily CO1π in character with some bonding contribution from CO5σ orbitals; the $8t_{1u}$ level is derived primarily from CO5σ orbitals, with bonding contributions from the Cr4p and CO2π orbitals and antibonding contributions from CO1π orbitals; and the $9t_{1u}$ level is primarily CO2π in character, with antibonding contributions from the CO5σ orbitals. Note that the outermost radial nodes in the Cr4s and 4p orbitals are well removed from the Cr core, giving the $8a_{1g}$ and $8t_{1u}$ orbitals the superficial appearance of Cr–C antibonding orbitals.

The accuracy of the calculated CO and $Cr(CO)_6$ occupied MO's may be assessed by comparison of calculated transition state ionization energies with experimental vertical ionization energies (see Tables I and II). Experimental 21.1 eV He(I) photoelectron bands are in general well resolved[10,11] and may be interpreted unambiguously with the exception of the $Cr(CO)_6$ 13–16 eV region. Here, comparison of detailed band structure obtained by different workers reveals a lack of consistency. In each case, however, three general features are evident: a narrow band at 13.4 eV and a more intense, broad, unsymmetric band at about 14 eV which has a broad shoulder at 14.5–15.5 eV. The broad 14 eV band arises from $Cr(CO)_6$ levels having CO 1π character, the 13.4 eV band arises from the $8t_{1u}$ (primarily CO5σ) level, and the 14.5–15.5 eV shoulder arises from the 5eg (CO5σ + Cr3d) and $8a_{1g}$ (primarily CO5σ) levels. Note that the different orbital characters of the levels responsible for the three features are reflected in the different relative band intensities obtained in the 40.8 eV He(II) spectrum.[11b] In the He(II) spectrum, the 14 eV band is far more intense than the 13.4 eV band and intensity in the 14.5–15.5 region equals that at 14 eV. Although several workers have attempted detailed interpretation of similar intensity variations in terms of MO character,[12] we feel that such analysis is unwarranted in the absence of angularly resolved spectra[11e] and calculated intensity data. Instead, we merely wish to point out that the relative intensity variations support the assignment of the 13–16 eV region to three features originating from levels having distinct MO character. Note that the photoelectron data are also consistent with an orbital ordering scheme where the $5e_g$ level lies above the CO 1π derived levels (see below).

The overall ordering of unoccupied orbitals in $Cr(CO)_6$ can be evaluated by comparison of experimental ultraviolet absorption energies[13] with calculated spin restricted transition state energies as shown in Table III. Most of our assignments, except for the two lowest energy absorptions, are in agreement with those of Beach and Gray.[13] The intense absorptions at 5.48 and 4.44 eV are assigned to the orbitally allowed $2t_{2g} \rightarrow 2t_{2u}$ and $2t_{2g} \rightarrow 9t_{1u}$ charge transfer transitions, respectively. The latter transition is weaker since the $9t_{1u}$ has appreciable

Table III. Calculated and Observed Electronic Transition Energies in $Cr(CO)_6$

Transition[a]	Energy, eV Calcd[b]	Obsd[c]
$2t_{2g} \rightarrow 2t_{1g}$ (2π)	5.9	6.31 (3.5)
$2t_{2g} \rightarrow 10t_{1u}$ (p)*	5.2	
$2t_{2g} \rightarrow 2t_{2u}$ (2π)*	4.8	5.48 (230)
$2t_{2g} \rightarrow 6e_g$ (d)	4.6	
$2t_{2g} \rightarrow 3t_{2g}$ (2π)	4.3	4.83 (3.7)
$2t_{2g} \rightarrow 9t_{1u}$ (2π)*	3.9	4.44 (25)
$2t_{2g} \rightarrow 9a_{1g}$ (s)	3.8	3.91 (3.7)
		3.60 (0.84)

[a] The predominantly metal or ligand character of the excited state orbital is indicated in parentheses. Symmetry allowed transitions are followed by asterisks. [b] Spin restricted transition state energy. [c] From ref 13, using the relation[8] 1 eV = 8065.5 cm^{-1}. Oscillator strengths are given in parentheses.

$CO5\sigma$ and Cr4p character. The weak 6.31 and 4.83 eV absorptions are assigned to the orbitally forbidden $2t_{2g} \rightarrow 2t_{1g}$ and $2t_{2g} \rightarrow 3t_{2g}$ transitions, respectively. Two metal to metal transitions calculated at 5.2 and 4.6 eV are obscured by the $2t_{2g} \rightarrow 2t_{2u}$ transition. The two lowest energy absorptions are assigned to vibration components of the $2t_{2g} \rightarrow 9a_{1g}$ metal to metal transition. A considerable body of experimental data,[14] however, is consistent with assignment of these lowest energy absorptions to the $2t_{2g} \rightarrow 6e_g$ transition. The present calculations could very well be in error on this assignment since the $9a_{1g}$ level, having considerable charge in the outer sphere region, should make the $2t_{2g} \rightarrow 9a_{1g}$ transition energy quite sensitive to environmental effects. Comparison of solution and gas phase data, however, does not bear out this prediction. The origin of the apparent error can be easily explained. If the Xα-MSW calculation has slightly overestimated the $Crd\sigma$-$CO5\sigma$ interaction and thus produced a $5e_g$ bonding orbital which lies slightly too low in energy (<1 eV), the corresponding $6e_g$ antibonding orbital will lie about 1 eV too high. Such a readjustment of the $5e_g$ and $6e_g$ levels would not alter significantly the relative strengths of metal-ligand σ and π bonding discussed above. This ambiguity could be resolved by carrying out spin unrestricted transition state energy and intensity calculations, and also by more fully resolving the photoelectron spectra in the 13-16 eV region.

Discussion

Traditionally, the transition metal-carbon monoxide bond has been viewed in terms of a synergic model where ligand to metal σ donation from the $CO5\sigma$ orbital is balanced by metal to ligand π back-donation into the $CO2\pi$ orbital.[15,16] This model is derived largely from the observation that the C-O bond distance d_{CO} increases and the C-O vibrational frequency νCO decreases upon complexation to a transition metal. Although the relative magnitudes of σ and π bonding have been disputed, formulations of the synergic model are invariably based on two assumptions: (1) that σ donation from the $CO5\sigma$ orbital implies a shortening of d_{CO} and an increase in νCO since the $CO5\sigma$ orbital is antibonding, whereas back-donation into the antibonding $CO2\pi$ orbital has the opposite effect, and (2) that σ bonding interactions must be about equal to π bonding interactions if approximate electroneutrality is to be achieved. The traditional synergic bonding model is consistent with many physical observations. It must be pointed out for future reference, however, that vibrational interaction constants[17] for $Cr(CO)_6$ are claimed to be inconsistent with this model.[18]

The present calculations as described above imply a bonding model in $Cr(CO)_6$ where M-C bonding is predominantly σ in character with only a small π contribution. Before presenting physical data which uniquely support this contention, we shall reevaluate the assumptions implicit in the traditional synergic model. First, the assumption that σ donation strengthens the CO bond whereas π bonding weakens the bond. The dependence of d_{CO} and ν_{CO} on orbital configuration in free CO can be evaluated using data given in Table IV. When an electron is removed from a 5σ orbital forming either CO^+ $X^2\Sigma^+$ or a CO Rydberg state $B^2\Sigma^+$, a very slight shortening of d_{CO} (0.013 and 0.008 Å, respectively) occurs, accompanied by slight changes in ν_{CO} (+41 and −61 cm^{-1}, respectively). When a 5σ electron is placed into a 2π orbital yielding the $A^1\pi$ and a $^3\pi$ states, substantial increases in d_{CO} (+0.107 and +0.078 Å, respectively) occur, accompanied by equally substantial changes in ν_{CO} (−645 and −428 cm^{-1}, respectively). In short, the $CO5\sigma$ orbital is for all practical purposes a nonbonding orbital whereas the $CO2\pi$ orbital is strongly antibonding, and as a result, strong Cr-Cσ bonding implies little regarding d_{CO} and ν_{CO} whereas even weak Cr-Cπ bonding may have significant impact upon d_{CO} and ν_{CO}.

Table IV. Bond Distances and Stretching Frequencies in Carbon Monoxide[a]

Species	Confign	State	d_{CO}, Å	ν_{CO},[b] cm^{-1}
CO	$(5\sigma)^2$	$X^1\Sigma^+$	1.128	2143
CO^+	$(5\sigma)^1$	$X^2\Sigma^+$	1.115	2184
CO[c]	$(5\sigma)^1 \ldots (7\sigma)^1$	$B_1\Sigma^+$	1.120	2082
CO	$(5\sigma)^1(2\pi)^1$	$A^1\pi$	1.235	1489
		$a^3\pi$	1.206	1715

[a] Data from ref 19. [b] $\nu_{0\leftarrow 1}$. [c] Data for the $b^3\Sigma^+$ state are not available.

Next, we turn to the traditional assumptions regarding the synergic nature to M-C bonding, where in order to preserve electroneutrality, it is assumed that σ interactions must be compensated by π interactions having comparable magnitude. From the shape of the $CO5\sigma$ orbital (see Figure 1), it is clear that substantial electron density is displaced away from the carbon end of the molecule. The same feature is observed in the $CO2\pi$ orbital to a far lesser extent. Thus when Cr-C bonding occurs and charge is concentrated in the region between Cr and C, a weak π interaction is able to charge-compensate for strong σ interaction, since $Crd\pi$ to $CO2\pi$ bonding leads so far more charge transfer than $CO5\sigma$ to $Crd\sigma$ bonding of an equivalent magnitude. This pattern of charge transfer may be qualitatively verified by examining the charge distributions in the $Cr(CO)_6$ $2t_{2g}$ and $5e_g$ orbitals given in Table II. About 20% of the charge in the $2t_{2g}$ level resides on CO, reflecting π back-donation, whereas comparison of the $(CO)_6$ $5e_g$ orbital with the $Cr(CO)_6$ $5e_g$ orbital shows about 20% loss of charge from CO as a result of σ donation. Owing to the higher degeneracy of the $2t_{2g}$ π bonding level relative to the $5e_g$ level, there is if anything a net flow of charge from metal to carbon in spite of the greater strength of the σ interaction. One must not, however, give quantitative meaning to such observations, since much charge redistribution occurs in the intersphere region, and sphere sizes differ slightly in the $(CO)_6$ and $Cr(CO)_6$ calculations.

Vibrational displacement interaction coordinates for $Cr(CO)_6$ reported by Jones[17] provide the most convincing physical evidence for the predominantly σ character of the Cr-C bond. The interaction coordinate $(j)_i$ gives the relative changes in the jth bond length resulting from stretching of the ith bond, a positive value indicating a weakening of the jth bond and a negative value indicating a strengthening. In the following discussion, bonds will be identified using this labeling scheme:

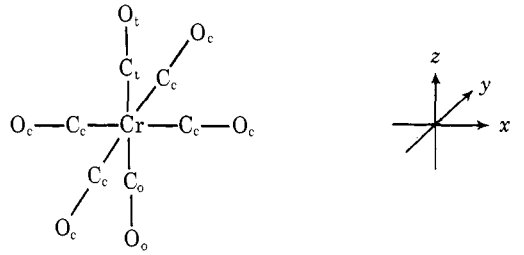

When a Cr-C bond is stretched, the effect on the C-O and remaining Cr-C bonds is defined by the interaction coordinates $(C_o\text{-}O_o)_{Cr\text{-}C_o} = -0.0446$, $(C_t\text{-}O_t)_{Cr\text{-}C_o} = +0.019$, $(C_c\text{-}O_c)_{Cr\text{-}C_o} = +0.0040$, $(Cr\text{-}C_t)_{Cr\text{-}C_o} = -0.228$, and $(Cr\text{-}C_c)_{Cr\text{-}C_o} = +0.0041$. The relative changes in C-O bond lengths resulting from a stretching of a Cr-C bond reflect the fact that C-O bond strength is affected predominantly by Cr-C π, not σ, bonding.[18] The relative changes in Cr-C bond lengths, however, are almost entirely trans directed, a fact which is inconsistent with substantial π contribution to total Cr-C bond order.[18] On the contrary, it demonstrates the predominantly σ character of the Cr-C bond. Stretching of the Cr-C_o bond in $Cr(CO)_6$ leads to C_{4v} molecular symmetry where the $d_{x^2-y^2}$ and d_{z^2} metal $d\sigma$ orbitals are orthogonal and no longer degenerate. Since trans Cr-C_t σ bonding involves only participation of the d_{z^2} orbital, participation of the $d_{x^2-y^2}$ orbital being symmetry forbidden, and cis Cr-C_c σ bonding involves principally the $d_{x^2-y^2}$ orbital, substantial perturbation of the Cr-C_t bond and only slight perturbation of the Cr-C_c bond is anticipated and observed when Cr-C_o is weakened.

We turn now to comparison of the $Cr(CO)_6X\alpha$-MSW calculation reported here with the HF-LCAO calculation reported by Hillier and Saunders[2a] and the HSF-DV calculation reported by Baerends and Ros.[2b] These two calculations yield molecular orbital eigenvalue orderings which are identical except for the position of the $8a_{1g}$ level, which lies below the CO 1π derived levels in the HF-LCAO calculation and lies in the same range as the CO 1π derived levels in the HFS-DV calculation. In contrast to the Xα-MSW calculation, the HF-LCAO and HFS-DV calculations yield a large (>1 eV) separation between the $7a_{1g}$ level and the remaining CO 4σ derived levels. This result is clearly inconsistent with photoelectron data. The overall ordering of levels in these two calculations is otherwise identical with that shown in Figure 3, except for the location of the $5e_g$ level which lies above the CO 1π derived levels in the HF-LCAO and HFS-DV calculations. As mentioned above, this location is consistent with photoelectron data.

A final item of interest is the relevance of the present study to binding of CO on metal surfaces. Considerable experimental and theoretical effort has been focused on the degree of interaction of the CO 5σ orbital with transitional metal surfaces evidenced by the relative ionization energies of the perturbed CO 5σ orbital and the relatively unperturbed CO 1π orbital.[20] In $Cr(CO)_6$, the energy of the Cr$d\sigma$-CO5σ $5e_g$ bonding orbital relative to the free CO 5σ level is the result of two opposing interactions: ligand-ligand antibonding interactions and metal-ligand bonding interactions (see Figure 3). In the absence of such ligand-ligand interactions on a metal surface, one would expect a more pronounced crossing of the CO 5σ and CO 1π derived levels.

Acknowledgment. We are deeply indebted to Professor K. H. Johnson for numerous helpful discussions.

References and Notes

(1) M. Elian and R. Hoffmann, *Inorg. Chem.*, **14**, 1058 (1975), and references cited therein.
(2) For representative calculations see (a) I. H. Hillier and V. R. Saunders, *Mol. Phys.*, **22**, 1025 (1971); (b) E. J. Baerends and P. Ros, *ibid.*, **30**, 1735 (1975); (c) J. Demuynck and A. Veillard, *Theor. Chim. Acta*, **28**, 241 (1973); (d) I. H. Hillier and V. R. Saunders, *Chem. Commun.*, 642 (1971); (e) H. B. Jansen and P. Ros, *Theor. Chim. Acta*, **34**, 85 (1974).
(3) (a) K. H. Johnson, *Adv. Quantum Chem.*, 7, 143 (1973); (b) *Annu. Rev. Phys. Chem.*, **26**, 39 (1975).
(4) (a) N. Roesch, W. G. Klemperer, and K. H. Johnson, *Chem. Phys. Lett.*, **23**, 149 (1973); (b) J. G. Norman, *Mol. Phys.*, **31**, 1191 (1976).
(5) O. R. Gilliam, C. M. Johnson, and W. Gordy, *Phys. Rev.*, **78**, 140 (1950).
(6) A. Whitaker and J. W. Jeffrey, *Acta Crystallogr.*, **23**, 977 (1967).
(7) K. Schwarz, *Phys. Rev. B*, **5**, 2466 (1972).
(8) R. C. Weast, Ed., "Handbook of Chemistry and Physics", 56th ed, CRC Press, Cleveland, Ohio, 1975, p F-235.
(9) In both calculations, $-2T/V$ could be more fully optimized by altering sphere radius ratios, thus changing the magnitudes of the eigenvalues without altering the spacing between eigenvalues significantly.
(10) For UV PES of CO see D. W. Turner and D. P. May, *J. Chem. Phys.*, **45**, 471 (1966).
(11) UV PES of $Cr(CO)_6$ have been measured by (a) D. W. Turner, C. Baker, A. D. Baker, and C. R. Brundle, "Molecular Photoelectron Spectroscopy", Wiley-Interscience, New York, N.Y., 1970, p 370; (b) B. R. Higginson, D. R. Lloyd, P. Burroughs, D. M. Gibson, and A. F. Orchard, *J. Chem. Soc., Faraday Trans. 2*, **69**, 1659 (1973); (c) B. R. Higginson, D. R. Lloyd, J. A. Connor, and I. H. Hillier, *ibid.*, **70**, 1418 (1974); (d) W. C. Price, unpublished data; (e) E. W. Plummer, unpublished data.
(12) See, for example, W. C. Price, A. W. Potts, and D. G. Streets in "Electron Spectroscopy", D. A. Shirley, Ed., North-Holland Publishing Co., Amsterdam, 1972, p 187.
(13) N. A. Beach and H. B. Gray, *J. Am. Chem. Soc.*, **90**, 5713 (1968).
(14) C. J. Ballhausen and H. B. Gray in "Coordination Chemistry", Vol. I, A. E. Martell, Ed., Van Nostrand-Reinhold, Princeton, N.J. 1971, pp 59–64.
(15) F. A. Cotton and G. Wilkinson, "Advanced Inorganic Chemistry", 3rd ed, Wiley-Interscience, New York, N.Y., 1972, pp 683–701, and references cited therein; L. Malatesta and S. Cenini, "Zerovalent Compounds of Metals", Academic Press, New York, N.Y., 1974, pp 1–60, and references cited therein.
(16) M. B. Hall and R. F. Fenske, *Inorg. Chem.*, **11**, 1619 (1972).
(17) L. H. Jones, *J. Mol. Spectrosc.*, **36**, 398 (1970).
(18) L. H. Jones and B. I. Swanson, *Acc. Chem. Res.*, **9**, 128 (1976).
(19) P. H. Krupenie, *Natl. Stand. Ref. Data Ser., Natl. Bur. Stand.*, **No. 5** (1966).
(20) D. R. Lloyd, C. M. Quinn, and N. V. Richardson, *Solid State Commun.*, **20**, 409 (1976), and references cited therein.